

Energy-Based Optimization of Physical-Layer Challenge-Response Authentication with Drones

Francesco Ardizzon¹, Damiano Salvaterra¹, Mattia Piana¹, and Stefano Tomasin^{1,2}

¹Department of Information Engineering, University of Padova, Italy

²Department of Mathematics, University of Padova, and CNIT, Parma, Italy

Abstract—Drones are expected to be used for many tasks in the future and require secure communication protocols. In this work, we propose a novel physical layer authentication (PLA)-based challenge-response (CR) protocol in which a drone Bob authenticates the sender (either on the ground or air) by exploiting his prior knowledge of the wireless channel statistic (fading, path loss, and shadowing). In particular, Bob will move to a set of positions in the space, and by estimating the attenuations of the received signals he will authenticate the sender. We take into account the energy consumption in the design and provide three solutions: a purely greedy solution (PG), an optimal Bellman iterative solution (BI), and a heuristic solution based on the evaluation of the standard deviation of the attenuations in the space. Finally, we demonstrate the effectiveness of our approach through numerical simulations.

I. INTRODUCTION

Nowadays, drones are being used for various tasks such as precision agriculture and disaster management. Moreover, the integration of drones in machine-to-machine communication is helpful in a variety of contexts, such as the Internet-of-Drones (IoD) [1] and non-terrestrial networks (NTN) [2]. However, these capabilities also make drones possible targets of attacks, including, for instance, spoofing to disrupt the drone's navigation system [3], [4], and jamming as a denial of service. Security threats and countermeasures for drone communications have recently been reviewed in [5].

This paper addresses the problem of drone authentication, where a drone, Bob, communicates with a transmitter Alice on the ground, while a third *intruder* agent, Trudy, aims to impersonate Alice and send fake malicious messages to Bob. The goal of Bob is to verify the authenticity of the sender and distinguish Alice from Trudy.

A classical authentication strategy is the (cryptography-based) challenge-response (CR) protocol, which is based on a secret key shared between Alice and Bob [6, Sec. 13.5]. In this protocol, the verifier sends a request, called a *challenge*, which only a legitimate user with a valid key can correctly answer. In this paper, we consider physical layer authentication (PLA)-based CR solutions first introduced in [7]. CR-PLA is based on *partially controllable channels* as the verifier Bob authenticates Alice by manipulating the channel and verifying that the received signal is consistent with the expected change.

This work was partially funded by the European Commission through the Horizon Europe/JU SNS project ROBUST-6G (Grant Agreement no. 101139068). Corresponding author: Francesco Ardizzon, email: francesco.ardizzon@unipd.it.

The change induced by Bob corresponds to the *challenge* of crypto-based CR. On the other hand, since the channel change is randomly decided by the verifier, it is difficult for Trudy to predict Bob's manipulations and the resulting channel. The advantages of such a class of protocols are detailed in [7].

In this paper, we propose a CR-PLA protocol for drone authentication, where the controllable parameter used as the challenge is the drone's position which impacts the path loss of the resulting wireless link. Even a sophisticated Trudy (which can freely tune its transmission power and pre-compensate the Trudy-Bob channel) that does not know the current drone's position has high uncertainty on the legitimate channel, strengthening the authentication procedure. In this scenario, the attacker's probability of success depends on the variability of the attenuation over the space of movement of Bob. Thus, we use the shadowing effect as a source of randomness. In particular, Bob checks whether the received response matches the distribution of attenuation due to shadowing given his position. Since more positions can be associated with the same (quantized) path loss and shadowing (i.e., the challenge), we propose an energy-saving CR-PLA strategy that minimizes the long-term energy expended by Bob while ensuring a target security level.

In [8], the authors proposed a CR-PLA protocol for drone communications. However, the channel was only partially modeled (e.g., no shadowing was considered), and the problem of energy minimization was not addressed.

In detail, the contributions of the paper are the following:

- a novel CR-PLA protocol for drone authentication using the channel shadowing.
- a verification procedure that is resilient to noise, e.g., due to fading and signal processing errors.
- a policy to minimize the long-term energy spent by the drone without compromising security. In detail, we propose a purely greedy solution (PG), an optimal Bellman iterative solution (BI), and a heuristic solution based on the standard deviation (STD) of attenuations in the space.

The rest of the paper is organized as follows. Section II introduces the system model. Section III analyzes the security of the proposed CR-PLA protocol, while the policy designs for energy minimization are discussed in Section IV. In Section V we show the numerical results. Finally, Section VI draws the conclusions.

II. SYSTEM MODEL

We consider the scenario of Fig. 1, where a drone (agent Bob), is communicating with a static (ground or aerial) device (agent Alice) while moving on a gridded region of points $\mathcal{X} = \{\bar{x}_1, \dots, \bar{x}_N\}$, where \bar{x}_n is the coordinate vector of position n . The drone receives messages from the ground device, including those for navigation and the instructions required by the mission (e.g., about when taking pictures). We design an authentication mechanism to ensure that the drone processes only messages coming from Alice, rather than from one impersonating her, Trudy. In turn, Trudy aims to impersonate Alice by sending messages to Bob purposely designed to be confused with those of Alice. Such messages aim for example to detour the drone from its designed route.

In the next part of this Section, we describe the channel model, the channel estimation, the threat model, and the model of drone power consumption.

A. Channel Model and Estimation

Transmissions are narrowband and channel gains are the result of (free space) path-loss, shadowing, and fading phenomena, which properly capture the main components of wireless propagation. As we are considering shadowing and path-loss as authentication features, our solution is independent of the number of antennas of each device.

As described in the next Section, Bob needs to estimate the channel over which the receiver message went through for CR-PLA. Several well-known strategies can be used for such a task, e.g., the least squares estimation. In particular, from the received signal Bob extracts the attenuation measured in dB [9]

$$a = \underbrace{a_{\text{PL}} + a_{\text{SH}}}_{\eta} + a_{\text{FD}}, \quad (1)$$

which includes the free space path-loss attenuation a_{PL} (modeled by the Friis formula), the shadowing attenuation a_{SH} , and fading attenuation a_{FD} . We also assume the transmit power of Alice and antenna gains of the legitimate agents are publicly known, and thus they can be ignored in our model.

Shadowing includes the effects of obstacles placed between the transmitter and receiver, thus $a_{\text{SH}} \sim \mathcal{N}(0, \sigma_{\text{SH}}^2)$ has a normal distribution (in dB scale) with standard deviation σ_{SH} .

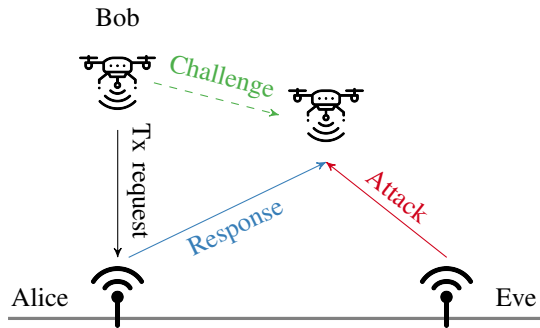


Fig. 1. Example of CR protocol.

Typical values are $\sigma_{\text{SH}} \in [4, 12]$ dB. The shadowing term depends on the location of the transmitter and the receiver, and channel gains of couples of transceivers in proximity have a high correlation. To model such a phenomenon, we resort to the well-known Gudmundson [9] model of the correlation of the shadowing components for two receivers at a distance Δ

$$r_{\text{SH}}(\Delta) = \sigma_{\text{SH}}^2 \exp\left(-\frac{\Delta}{D_{\text{coh}}}\right), \quad (2)$$

where D_{coh} is the coherence distance. Typical values of the coherence distance range from 3λ to 20λ (where λ is the wavelength) in an urban area with many obstacles and a flat rural area [9], respectively.

Fading accounts for shorter channel variations and depends on Doppler spread and multipath. As it is hardly predictable, it cannot be exploited in our authentication scheme. Shadowing instead is shown to have a higher coherence distance. Moreover, it varies only slowly over time (i.e., slow fading). Thus, we will exploit the shadowing for the CR protocol while considering fading as estimation noise.

B. Threat Model

Concerning the attacker Trudy, we assume that she can control her transmitting signal to induce any desired attenuation at Bob. On the other hand, we assume Bob's position to be unknown to her until signal reception, i.e., the spoofing signal does not depend on Bob's position.

C. Power Consumption for Movements

Since the protocol requires the drone to move, we define $\epsilon(\mathbf{x}, \mathbf{x}')$ as the energy needed to move from position \mathbf{x} to position \mathbf{x}' . Following the results in [10], the energy consumption (in Joule) for both vertical and horizontal movement follows the model

$$\epsilon(\mathbf{x}, \mathbf{x}') = \alpha_1 \frac{\|\mathbf{x} - \mathbf{x}'\|}{V} - \alpha_0, \quad (3)$$

where V is the (constant) drone velocity. For instance, taking $\alpha_1 \approx 308.71$ J/s and $\alpha_0 \approx 0.85$ J, (3) fits the energy consumption when performing an horizontal movement.

III. CHALLENGE-RESPONSE AUTHENTICATION AT THE PHYSICAL LAYER

Bob aims to distinguish if the received messages come from Alice or Trudy. Additionally, as we work with an energy-limited device, we aim to minimize Bob's movements to lower the energy consumption in the long run.

We propose an authentication mechanism based on the attenuation measured by Bob on the received message compared to the one expected according to the current positions of Alice and Bob. In particular, we let Bob choose a position \mathbf{x} , and such choice is considered to be the challenge in a CR protocol. In turn, the attenuation measured when in such a position is the response. The position and thus the challenge shall be chosen taking into account security, therefore it has to guarantee low false alarm (FA) and missed detection (MD) probabilities when testing the authenticity of the response while keeping the

energy consumption as low as possible. The position is chosen also to minimize the movements, thus keeping under control the drone power consumption.

We assume that Bob has a *map* of quantized attenuations over the grid \mathcal{X} . In particular, indicating with $q(\cdot)$ the quantization function, we have $\hat{a}(\bar{\mathbf{x}}_n) = q(\eta(\bar{\mathbf{x}}_n))$, where η is defined in (1) and includes only free-space path loss and shadowing, obtained by averaging out fading over multiple measurements. The set of the *unique* quantized attenuations is therefore $\mathcal{A} = \{a : \exists n : \hat{a}(\bar{\mathbf{x}}_n) = a\}$. Moreover, for any attenuation $a' \in \mathcal{A}$, let us define the set of positions all having the same attenuation as

$$\mathcal{X}_{a'} \triangleq \{\mathbf{x} \in \mathcal{X} | \hat{a}(\mathbf{x}) = a'\} . \quad (4)$$

The proposed authentication mechanism distinguishes between Alice's and Trudy's signals based on the prior knowledge of such a map.

In the following, we assume that a message is transmitted every integer time $t = 0, 1, \dots$ only to simplify notation. In practice, messages do not need to be sent at regular time.

The proposed CR-PLA-based algorithm is composed of the following steps, also shown in Fig. 1. At time t_0 the following occur

- 0) *Channel Measurements*: Bob moves on positions in \mathcal{X} while Alice transmits several pilot signals. These transmissions are authenticated by higher-layer security mechanisms, Bob uses them to obtain \mathcal{A} and \mathcal{X}_a , $a \in \mathcal{A}$.

Next, when Alice wants to transmit a message at time $t > t_0$,

- 1) *Challenge*: Alice transmits in broadcast a transmission request to Bob (Tx request in Fig. 1), who chooses uniformly at random an attenuation in \mathcal{A} , i.e., $a_t^* \sim \mathcal{U}(\mathcal{A})$. Then Bob moves to a position \mathbf{x}^* , for which $\hat{a}(\mathbf{x}^*) = a_t^*$. The selection of the position is discussed in Section IV.
- 2) *Response*: Alice transmits her message, including pilot signals to Bob.
- 3) *Verification*: Upon reception, Bob estimates the attenuation of the channel over which the message went, \tilde{a}_t and if it statistically matches a_t^* , the message is considered authentic otherwise is labeled as fake. The test procedure is presented in Section III-A.

We remark that this procedure does not make use of pre-shared keys, except during step 0. This is common also to the tag-based PLA mechanisms where it is assumed either that it is possible to perform a secure data collection, or as mentioned before, that the verifier knows the measurement distribution in advance.

Bob chooses a_t^* to be picked from \mathcal{A} using a uniform distribution: while several different choices are possible, this specific distribution will force Trudy to use a random guessing strategy, as we will detail in the next Section.

A. Authentication Verification Procedure

In Step 1, after the transmission request, Bob will move towards \mathbf{x}^* , stop, and wait for the signal from Alice.

In Step 3, due to the fading, hardware imperfections, and errors introduced by the signal processing, Bob will measure

an attenuation \tilde{a}_t instead of a_t^* . We frame the problem of checking whether \tilde{a}_t is a noise-corrupted version of a_t^* as a binary hypothesis testing. We consider \mathcal{H}_0 as the legitimate (null) hypothesis (see (1)), and \mathcal{H}_1 as the under-attack hypothesis, i.e.

$$\tilde{a}_t = \begin{cases} a_t^* + a_{\text{FD}} & \text{if } \mathcal{H}_0, \\ b_t & \text{if } \mathcal{H}_1, \end{cases} \quad (5)$$

where $a_{\text{FD}} \sim \mathcal{E}(1)$ is the exponential random variable (with parameter 1) describing the fading and b_t is the attenuation measured when under attack.¹ Notice that we are considering a worst-case scenario where Trudy can pre-compensate the channel to account for such noise and that when under attack, only Trudy's signal is received and Alice causes no interference.

Bob then checks whether \tilde{a}_t matches the statistic of the chosen challenge a_t^* . In binary hypothesis testing, the optimal strategy is to use the likelihood ratio test (LRT). Still, this test would require the knowledge of the attenuation when under attack, which is unknown a priori. Thus we resort instead to the likelihood test (LT), and defining $p(\tilde{a}_t | a_t^*, \mathcal{H}_0)$ the PDF of \tilde{a}_t under the hypothesis \mathcal{H}_0 the LT is

$$\text{LT}(\tilde{a}_t, \varphi) : p(\tilde{a}_t | a_t^*, \mathcal{H}_0) \leq \varphi \iff \mathbb{1}(\tilde{a}_t - a_t^*) \exp[-(\tilde{a}_t - a_t^*)] \leq \varphi, \quad (6)$$

where $\mathbb{1}(\cdot)$ is the Heaviside step function and φ is a threshold chosen by Bob to meet a predefined FA probability P_{fa} . Note that only inputs obtaining outputs greater than φ in (6) are considered authentic. Even if it has no general optimality guarantee, this test is often used in practice as it does not require any knowledge about the strategy employed by the attacker.

The LT (6) can be interpreted as a test of distance in the probability space. In particular, φ identifies an interval \mathcal{I} around a_t^* : only values falling inside \mathcal{I} , i.e., close to a_t^* are considered to be authentic. Then, a FA occurs when a legitimate \tilde{a}_t falls outside of \mathcal{I} , and, conversely, for a fixed FA probability, the interval size must be (by inverting the cumulative distribution function of the exponential random variable)

$$|\mathcal{I}| = -\ln P_{\text{fa}} . \quad (7)$$

On the other hand, a MD occurs when the attacker manages to pick a value b_t falling inside \mathcal{I} , thus close enough to a_t^* . Even a sophisticated attacker able to compensate the Trudy-Alice channel can only perform a random guessing attack $b_t \sim \mathcal{U}(\mathcal{A})$. Hence, the MD probability is due to the difference between the uniform random variables b_t and a_t^* defined over the same domain, which results in a triangular random variable, therefore the MD probability is

$$P_{\text{md}} = \frac{1}{2} - \frac{(r + \ln P_{\text{fa}})^2}{2r^2}, \quad (8)$$

where $r = \max_n \hat{a}(\bar{\mathbf{x}}_n) - \min_n \hat{a}(\bar{\mathbf{x}}_n)$.

¹Note that in (5) we ignored the effects of quantization, considering it negligible when compared to fading.

IV. ENERGY-AWARE MECHANISM OPTIMIZATION

In this section, we discuss the choice of the position \mathbf{x}^* selected by Bob for CR-PLA, taking into account both security (in terms of FA and MD probabilities) and energy consumption for the drone movement. In particular, assuming that we run the CR-PLA many times and that at $t = 0$ the drone starts from a random initial position in \mathcal{X} , we design a *policy* to choose the next position, which minimizes the overall energy spent at each time $t > 0$.

As previously pointed out, the protocol security is based on the statistic of the selected attenuation a_t^* and not on the actual Bob position. However, many positions may correspond to the same attenuation if the grid \mathcal{X} is dense enough. Hence, this opportunity can be exploited to minimize the energy consumption of the drone using the CR-PLA protocol.

We formalize the problem by modeling it as a Markov decision process (MDP). In detail, we introduce the *state* at step t as $s_t \triangleq \{\mathbf{x}_t, a_t^*\}$, where \mathbf{x}_t is the current position and a_t^* is the randomly picked attenuation. We define as *action* the next position to be taken when in state $s_t = \{\mathbf{x}_t, a_t^*\}$ leading the drone to one of the positions in the set $\mathcal{X}_{a_t^*}$. Then, the policy $\pi(s_t)$ maps state s_t to the next position, i.e.

$$\pi(s_t) = \mathbf{x}_{t+1}. \quad (9)$$

When passing from state s_t to state $s_{t+1} = \{\mathbf{x}_{t+1}, a_{t+1}^*\}$, we define the *instantaneous reward* from (3) as

$$R(s_t, s_{t+1}) = -\epsilon(\mathbf{x}_t, \mathbf{x}_{t+1}). \quad (10)$$

Note that the selection of a specific action at time t is not enough to determine the state at $t + 1$, since a_{t+1}^* is random and independent from \mathbf{x}_{t+1} .

Finally, we formally define the long-term optimization problem

$$\{\pi^*(s)\} = \operatorname{argmax}_{\{\pi(s)\}} E \left[\sum_{t=0}^{\infty} R(s_t, s_{t+1}) \right], \quad (11)$$

where the expectation $E(\cdot)$ is taken over both the states and the actions.

A. Bellman Iterative (BI) Solution

To solve the MDP, we resort to the Bellman equation and dynamic programming. In particular, the *value update* function is

$$V(s_t) = \frac{1}{|\mathcal{A}|} \sum_{\substack{s_{t+1} \\ \{\pi(s_t), a_{t+1}^*\}}} \underbrace{\left(R(s_t, s_{t+1}) + \sum_{a \in \mathcal{A}} \gamma V(s_{t+1}) \right)}_{R'(s_t, s_{t+1})}, \quad (12)$$

and the corresponding *policy update* is

$$\pi(s_t) = \frac{1}{|\mathcal{A}|} \operatorname{argmax}_{v: a(v)=a_t} \sum_{s_{t+1}=\{v, a_{t+1}^*\}} R'(s_t, s_{t+1}), \quad (13)$$

where $0 < \gamma < 1$ is the *discount factor*, chosen to balance greedy behaviors over later rewards. To solve the problem we

consider the Bellman iterative (BI) solution [11, Ch. 1], where at each step i we update the values as

$$V_{i+1}(s_t) = \frac{1}{|\mathcal{A}|} \max_{v: a(v)=a_t} \sum_{s_{t+1}=\{\pi(s_t), a_{t+1}^*\}} R'_i(s_t, s_{t+1}), \quad (14)$$

where $R'_i(s_t, s_{t+1})$ is computed using (12) with $V_i(s_{t+1})$. The procedure is repeated until either 1) a maximum predefined number of iterations is reached or 2) the right-hand side coincides with the left-hand side in (14).

In the worst-case scenario, the total computational cost is due to the total number of states, and the number of possible actions. More in detail, we have $M = N|\mathcal{A}|$ states, and, at most, $K \triangleq \max_{a^* \in \mathcal{A}} |\mathcal{X}_{a^*}|$ actions, leading to a total of $|\mathcal{A}|N^2MK$ computations in the worst case.

B. Purely Greedy (PG) Solution

The PG aims at minimizing the long-term cost by maximizing the instantaneous reward, i.e., the one requiring less energy to be reached. Given the position at time t , \mathbf{x}_t , the next position \mathbf{x}_{t+1} is the closest in $\mathcal{X}_{a_t^*}$. Formally,

$$\pi(s_t) = \operatorname{argmin}_{\mathbf{x}_{t+1} \in \mathcal{X}_{a_t^*}} \epsilon(\mathbf{x}_t, \mathbf{x}_{t+1}). \quad (15)$$

While easy to implement, such a solution is in general not optimal as it is not always true that by maximizing the instantaneous reward we maximize also the long-term reward.

C. Standard Deviation-based (STD-based) Solution

We now propose another heuristic approach that estimates the *strategic value* $Y(\mathbf{x})$ of each position $\mathbf{x} \in \mathcal{X}$, such strategic value evaluates how convenient is for the drone to pick one position over the other, and replaces the $V(s)$ computed by the BI solution. We thus have to design function $Y(\mathbf{x})$ and a proper policy.

Indeed, a position \mathbf{x} should be associated with a high value $Y(\mathbf{x})$ if several different attenuations can be found in its neighborhood, therefore it is highly probable that when in \mathbf{x} , the drone will get the required attenuation with movements to nearby positions, thus saving energy. To measure such diversity we consider the STD of attenuations in the neighborhood of each \mathbf{x} . In detail, let us introduce the set of $L \times L$ positions in \mathcal{X} closest to (and including) \mathbf{x} as $W_{\mathbf{x}}$. Next, we define the strategic value as

$$Y(\mathbf{x}) = \sqrt{\sum_{\mathbf{x}' \in W_{\mathbf{x}}} (a(\mathbf{x}') - \mu_{\mathbf{x}})^2}, \quad \mu_{\mathbf{x}} = \frac{1}{L^2} \sum_{\mathbf{x}' \in W_{\mathbf{x}}} a(\mathbf{x}'). \quad (16)$$

We remark that the computational cost to derive $Y(\mathbf{x})$ is NL^2 , which is much lower than that of $V(s)$.

Concerning the actual policy, while at the initial stage, getting the drone with the zone with high $Y(\mathbf{x})$ should have high priority, at later stages, we should already be in a zone with sufficiently high $Y(\mathbf{x})$, thus we could simply use the PG strategy. Thus, to balance such behaviors, at step t , we consider the following policy

$$\pi(s_t) = \operatorname{argmax}_{\mathbf{x}_{t+1} \in \mathcal{X}_{a_t^*}} \left\{ \delta e^{-t/\beta} Y(\mathbf{x}_{t+1}) - \epsilon(\mathbf{x}_t, \mathbf{x}_{t+1}) \right\}, \quad (17)$$

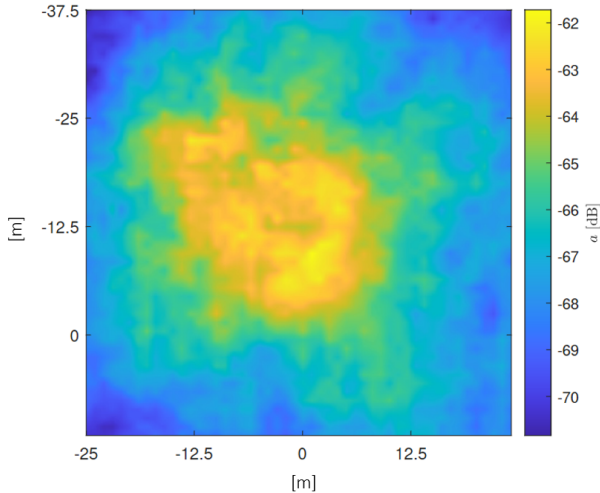


Fig. 2. Example of channel realization, including both free space path-loss and shadowing over region \mathcal{X} .

where δ is the normalization parameter that allows to balance reward and STDs, while β is a decaying factor. Indeed, at later rounds, policies (15) and (17) are equivalent. The optimization in (17) can be done by enumeration over \mathcal{X}_{a^*} .

V. NUMERICAL RESULTS

We report in this section the performance of the proposed protocol. We modeled a scenario where a drone moves around a plane area of size $50 \text{ m} \times 50 \text{ m}$ at a height of 20 m from the center of the plane area where Alice is. The free space path loss is modeled via the Friis formula. The area is sampled using a step size of 1 m along both directions, ending up with a total of $N = 2500$ sampled positions. The considered carrier frequency is $f_0 = 1.8 \text{ GHz}$. The shadowing coherence distance is $D_{\text{coh}} = 10\lambda$ with standard deviation $\sigma_{SH} = 6 \text{ dB}$, following the procedure reported in the Appendix. Fig. 2 shows a realization of the channel, which includes both free space path loss and shadowing. To make the BI solution computationally feasible, the quantizer $q(\cdot)$ is uniform with 10 levels. As expected, the minimum attenuation is obtained approximately at the center, where the distance between Alice and Bob is at its minimum. On the other hand, the shadowing may cause both constructive and destructive interference: for instance, we get a higher attenuation in the right than in the left corners of the map.

A. Security Performance

First, we assess the security performance of the protocol. Considering model (5), we set $r = 5, 10, 20,$ and 40 dB . Fig. 3 compares the detection error tradeoff (DET) curves obtained for different range values r considering both simulation and the analytical derivation (8). We confirm the validity of our model, as the analytical model and simulation results almost perfectly match. As expected, when r increases, it becomes harder for the attacker to guess the legitimate a^* , thus the P_{md} increases.

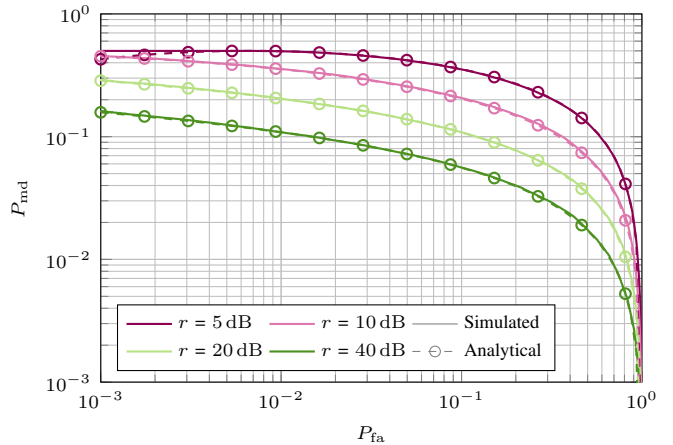


Fig. 3. DET curves of the proposed authentication procedure for different r values (in dB). Analytical (circles mark, dashed) vs simulated (continuous).

B. Energy Optimization

Next, we evaluate the results of the energy minimization policies described in Section IV. Concerning the parameters of such solutions, for BI we fixed the discount factor $\gamma = 0.95$; for the STD-based solution, we consider instead windows $W(\mathbf{x})$ of size $L = 5$, normalization factor $\delta = 100$, and decaying factor parameter $\beta = 20$.

Fig. 4 shows an example of 100 consecutive runs of the CR-PLA protocol. All the energy minimization policies start from the same random position. While all three strategies lead the drone to the same region, the PG takes much longer to get the drone to that region, with it initially straying on the lower part of the map. Conversely, both BI and STD-based solutions make the drones move a lot on the first step to get as soon as possible to the left corner. However, once there, the drone can stay locked in that advantageous region, with minimal movements. Thus, as designed, both strategies prioritize the long-term reward, at the expense of the instantaneous cost. The difference between BI and the STD-based solutions is barely recognizable, with the latter often superimposing over the first solution.

Fig. 5 shows the average consumed energy $E[\epsilon(\mathbf{x}_t, \mathbf{x}_{t+1})]$ as a function of t , after random initialization, obtained using the PG, the BI, and the STD-based approaches. As it can be seen from the magnification, on the first movements the greedy policy requires on average (slightly) less energy. However, after just a few steps, both BI, and the STD-based solutions outperform the PG solution, with a gap that increases over time. As expected, the best performance is achieved by the BI. Still, the gap between the optimal BI and the STD-based approach is limited. Thus, in scenarios where the MDP-based solution is not computationally feasible, it is reasonable to resort to the heuristic STD approach.

VI. CONCLUSIONS

We presented a novel CR-PLA protocol for drone communication. Using the previous knowledge of path loss, which includes modeling and sampling of free space path loss and

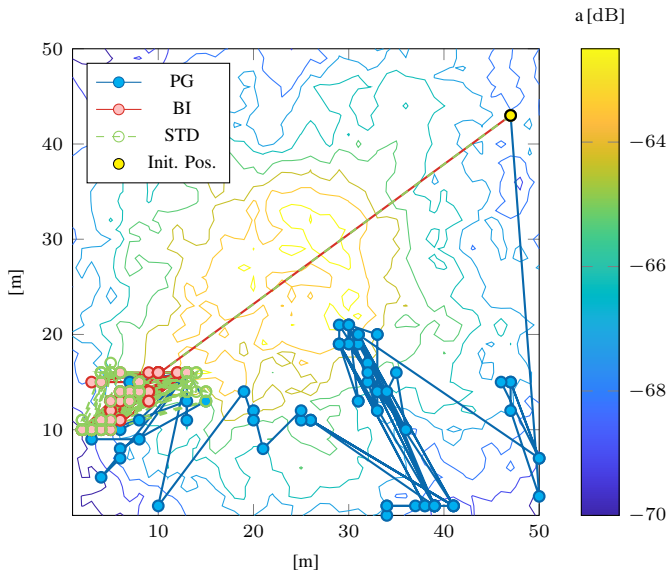


Fig. 4. Examples of trajectories obtained by using the PG (blue), the BI (red), and the STD-based approach (green). The contour plot shows $\hat{a}(\bar{x})$ in dB.

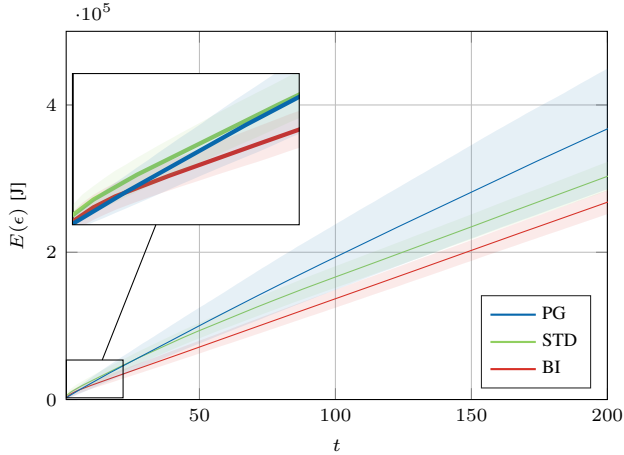


Fig. 5. Average consumed energy $E[\epsilon(\mathbf{x}_t, \mathbf{x}_{t+1})]$ vs t , using the PG (blue), the BI (red), and the STD-based approach (green). Average (continuous line) plus/minus standard deviation (shaded area).

shadowing, the drone manipulates the channel by moving on a specific position of the map. The verification procedure checks whether the measured path loss is consistent with the expected measurement. Additionally, the proposed protocol includes the long-term energy consumption in the design, while preserving the security of the system. Concerning the energy consumption minimization, three solutions have been considered: PG, BI, and STD-based. We compared the three solutions via numerical simulations, and a clear tradeoff between computational complexity and effectiveness in terms of energy consumed is observed.

REFERENCES

[1] M. Alam, N. Ahmed, R. Matam, and F. A. Barbhuiya, "IEEE 802.11ah-enabled Internet of drone architecture," *IEEE Internet of Things Mag.*, vol. 5, no. 1, pp. 174–178, Mar. 2022.

[2] X. Lin, S. Rommer, S. Euler, E. A. Yavuz, and R. S. Karlsson, "5G from space: An overview of 3GPP non-terrestrial networks," *IEEE Commun. Stand. Mag.*, vol. 5, no. 4, pp. 147–153, Oct. 2021.

[3] M. Ceccato, F. Formaggio, and S. Tomasin, "Spatial GNSS spoofing against drone swarms with multiple antennas and Wiener filter," *IEEE Trans. on Signal Proces.*, vol. 68, pp. 5782–5794, Oct. 2020.

[4] G. Michieletto, F. Formaggio, A. Cenedese, and S. Tomasin, "Robust localization for secure navigation of UAV formations under GNSS spoofing attack," *IEEE Trans. Autom. Sci. Eng.*, pp. 1–14, Sept. 2022.

[5] M. Adil, M. A. Jan, Y. Liu, H. Abulkasim, A. Farouk, and H. Song, "A systematic survey: Security threats to UAV-aided IoT applications, taxonomy, current challenges and requirements with future research directions," *IEEE Trans. Intell. Transp. Syst.*, vol. 24, no. 2, pp. 1437–1455, Feb. 2023.

[6] P. C. Gupta, *Cryptography and network security*. PHI Learning, 2014.

[7] S. Tomasin, H. Zhang, A. Chorti, and H. V. Poor, "Challenge-response physical layer authentication over partially controllable channels," *IEEE Commun. Mag.*, vol. 60, no. 12, pp. 138–144, Dec. 2022.

[8] F. Mazzo, S. Tomasin, H. Zhang, A. Chorti, and H. V. Poor, "Physical-layer challenge-response authentication for drone networks," in *Proc. IEEE Global Communications Conf.*, 2023.

[9] N. Benvenuto, G. Cherubini, and S. Tomasin, *Algorithms for Communications Systems and their Applications*, 2nd ed. Wiley, 2021.

[10] H. V. Abeywickrama, B. A. Jayawickrama, Y. He, and E. Dutkiewicz, "Comprehensive energy consumption model for unmanned aerial vehicles, based on empirical studies of battery performance," *IEEE Access*, vol. 6, pp. 58 383–58 394, Oct. 2018.

[11] E. Feinberg and A. Shwartz, *Handbook of Markov Decision Processes: Methods and Applications*. Springer, 2002.

APPENDIX

To model the shadowing effect we follow the procedure described in [9, Sec. 4.1.10]. First, we consider a regular $N_1 \times N_2$ 2D grid with equal step size A , \mathcal{X} . Each point of the grid (n_1, n_2) is mapped to a position \mathbf{x} , thus to an attenuation $\hat{a}(\mathbf{x}) = a(n_1, n_2)$. For simplicity, we consider $(0, 0)$ to be the center of the grid. Then, the distance from the center of point \mathbf{x} with coordinates (n_1, n_2) is

$$\Delta(\mathbf{x}) = A\sqrt{n_1^2 + n_2^2}. \quad (18)$$

Thus, considering the Gudmonson model for the autocorrelation function $r_{SH}(\Delta)$ (2), the associated power spectral density is

$$\mathcal{P}(\mathbf{x}) = \text{DFT}_2[r_{SH}(\Delta)] = \text{DFT}_2\left[r_{SH}\left(A\sqrt{n_1^2 + n_2^2}\right)\right], \quad (19)$$

where $\text{DFT}_2(\cdot)$ indicates the 2D discrete Fourier transform. Next, we generate a set of i.i.d. complex Gaussian samples, one for each point in the grid, $w \sim \mathcal{CN}(0, \sigma_{SH}^2)$. Then, the shadowing component $a_{SH}(\mathbf{x})$ is obtained by the 2D convolution

$$a_{SH}(\mathbf{x}) = \sum_{\mathbf{x}' \in \mathcal{X}} h_{sh}(\mathbf{x}') w(\mathbf{x} - \mathbf{x}'), \quad (20)$$

where the 2D filter impulse response is obtained as

$$\mathcal{H}_{sh}(\mathbf{x}) = \mathcal{K}\sqrt{\mathcal{P}(\mathbf{x})} \quad \text{and} \quad h_{sh}(\mathbf{x}) = \text{DFT}_2^{-1}[\mathcal{H}_{sh}(\mathbf{x})], \quad (21)$$

where \mathcal{K} is normalization coefficient chosen such that h_{sh} has unitary energy.